

Membrane fouling in osmotically driven membrane processes: A review

She, Qianhong; Wang, Rong; Tang, Chuyang Y.; Fane, Anthony Gordon

2016

She, Q., Wang, R., Fane, A. G., & Tang, C. Y. (2016). Membrane fouling in osmotically driven membrane processes: A review. *Journal of Membrane Science*, 499, 201-233.

<https://hdl.handle.net/10356/82800>

<https://doi.org/10.1016/j.memsci.2015.10.040>

© 2015 Elsevier B.V. This is the author created version of a work that has been peer reviewed and accepted for publication by *Journal of Membrane Science*, Elsevier. It incorporates referee's comments but changes resulting from the publishing process, such as copyediting, structural formatting, may not be reflected in this document. The published version is available at: [<http://dx.doi.org/10.1016/j.memsci.2015.10.040>].

Downloaded on 13 Mar 2024 15:50:10 SGT

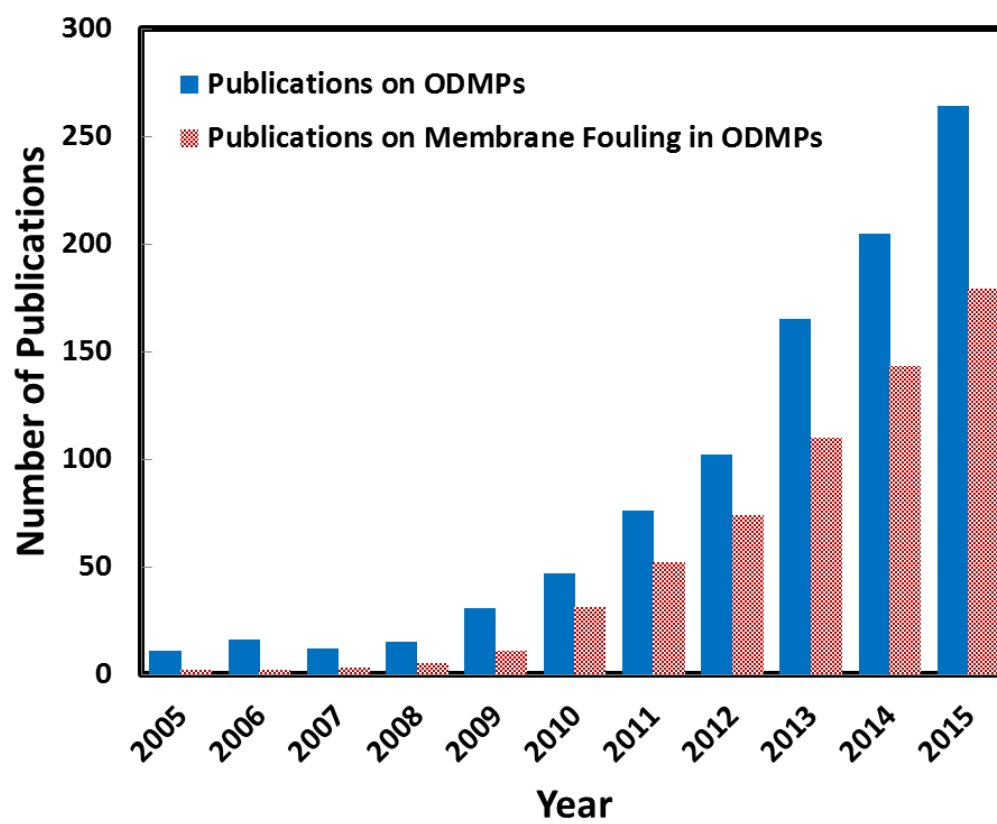
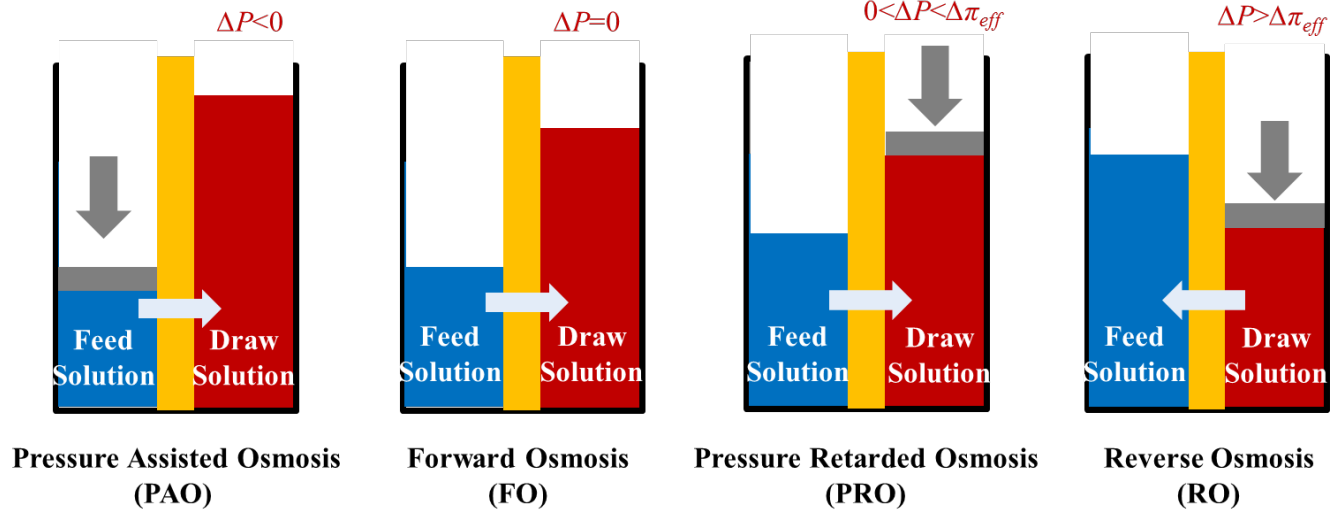
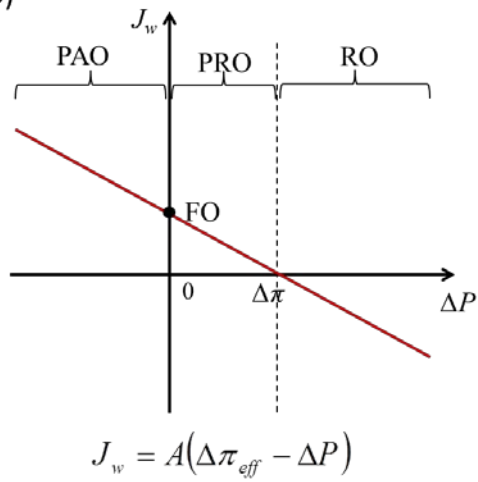


Figure 1. Annual number of publications on ODMPs and membrane fouling in ODMPs since 2005. Data were obtained from Scopus on 7th Oct 2015. Keywords for searching are “Forward Osmosis or Pressure Retarded Osmosis” and “Forward Osmosis or Pressure Retarded Osmosis and Fouling” respectively. In searched results, the document type does not include Short Survey, Erratum, Letter, Conference Review, and Conference Paper.

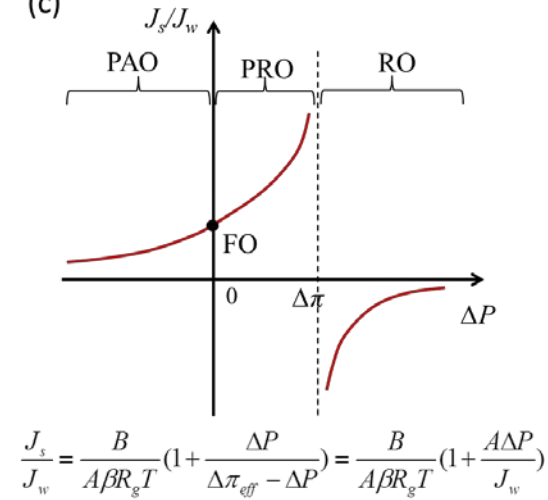
(a)



(b)



(c)



(d)

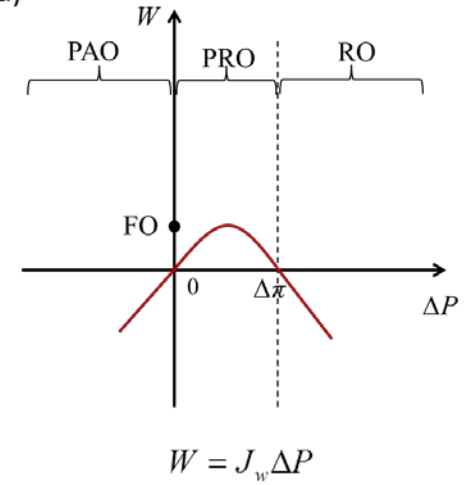


Figure 2. Classification and characteristics of osmosis-related membrane separation processes. (a) Direction of water flows in RO, PRO, FO and PAO processes. In RO, water flows from high salinity draw solution (DS) to low salinity feed solution (FS) driven by the applied hydraulic pressure; in PRO and FO, water flows from low salinity FS to high salinity DS driven by the osmotic pressure; in PAO, water flows from low salinity FS to high salinity DS driven by both osmotic pressure and applied hydraulic pressure. (b) Water flux (J_w) magnitude, (b) specific solute flux (J_s/J_w) magnitude, and (c) power density (W) magnitude as a function of applied pressure in RO, PRO, FO and PAO processes.

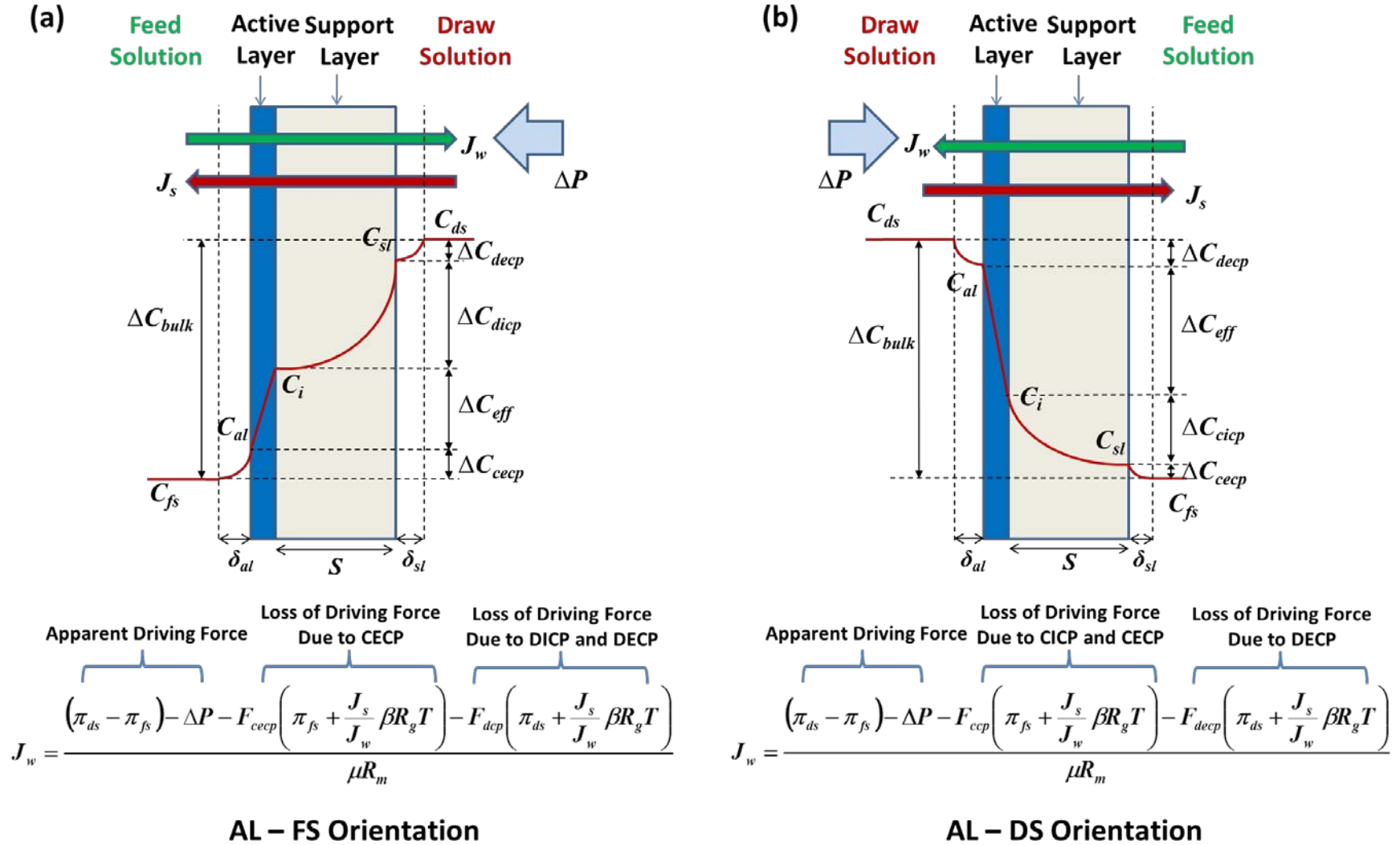


Figure 3. Schematic illustration of osmotic-resistance filtration model in ODMPs in (a) active-layer-facing-feed-solution (AL-FS) orientation and (b) active-layer-facing-draw-solution (AL-DS) orientation. All the driving forces represented by the concentration profile across the membrane due to ICP and ECP are specifically differentiated in accordance with the osmotic-resistance filtration model. The mathematic expressions of all the concentration polarization factors (F_{cep} , F_{decp} , F_{cicp} and F_{decip}) are described in Appendix

A. It is assumed that (1) the osmotic pressure is linearly proportional to the concentration and (2) the feed solution and draw solution contain the same solute.

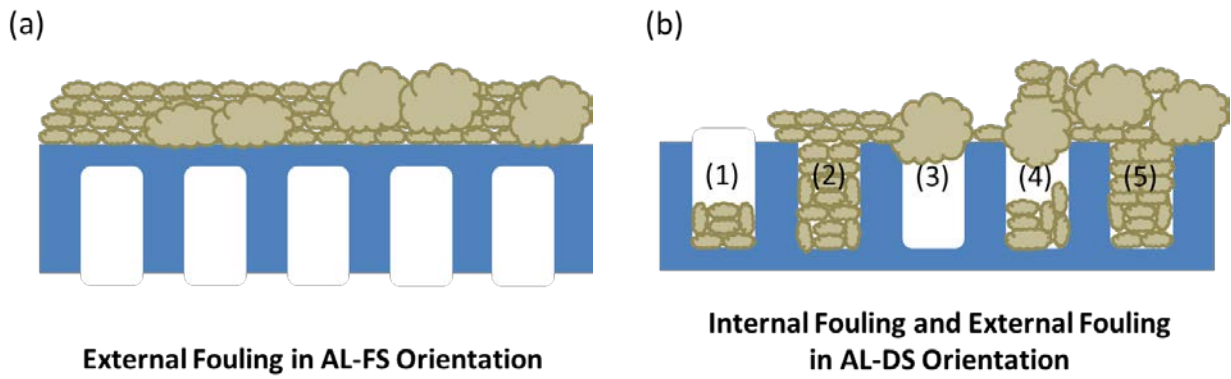
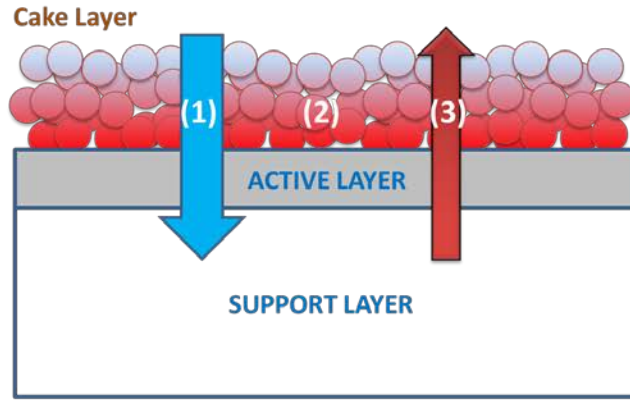


Figure 4. External fouling and internal fouling in ODMPs. (a) Only external fouling occurs in AL-FS orientation, (b) both external fouling and internal fouling occur in AL-DS orientation.

(a)

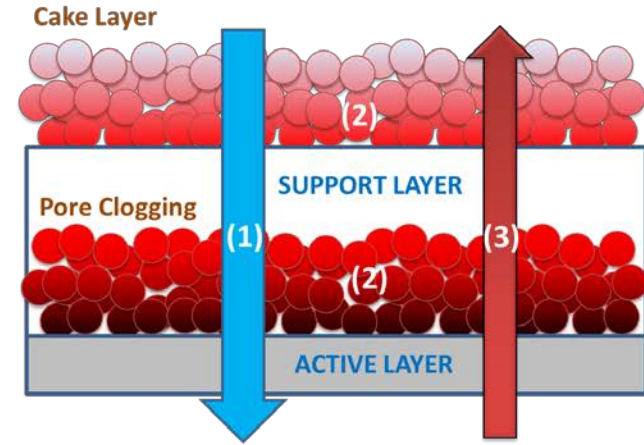
**AL-FS Orientation**

$$J_{w,f} = \frac{(\pi_{ds} - \pi_{fs}) - \Delta P - F_{cep,f} \left(\pi_{fs} + \frac{J_{s,f}}{J_{w,f}} \beta R_g T \right) - F_{dep,f} \left(\pi_{ds} + \frac{J_{s,f}}{J_{w,f}} \beta R_g T \right)}{\mu (R_m + R_f)}$$

(1) Additional hydraulic resistance (R_f)

(2) Cake-enhanced CP in AL-FS orientation ($F_{cep,f} > F_{cep}$)
Cake-enhanced ECP & Pore-clogging enhanced ICP in
AL-DS orientation ($F_{cep,f} > F_{cep}$)

(b)

**AL-DS Orientation**

$$J_{w,f} = \frac{(\pi_{ds} - \pi_{fs}) - \Delta P - F_{cep,f} \left(\pi_{fs} + \frac{J_{s,f}}{J_{w,f}} \beta R_g T \right) - F_{dep,f} \left(\pi_{ds} + \frac{J_{s,f}}{J_{w,f}} \beta R_g T \right)}{\mu (R_m + R_f)}$$

(3) Change of rejection property ($J_{s,f}/J_{w,f}$)

Figure 5. Schematic illustration of the influence of membrane fouling on water flux behavior in ODMs according to the osmotic-resistance filtration model.

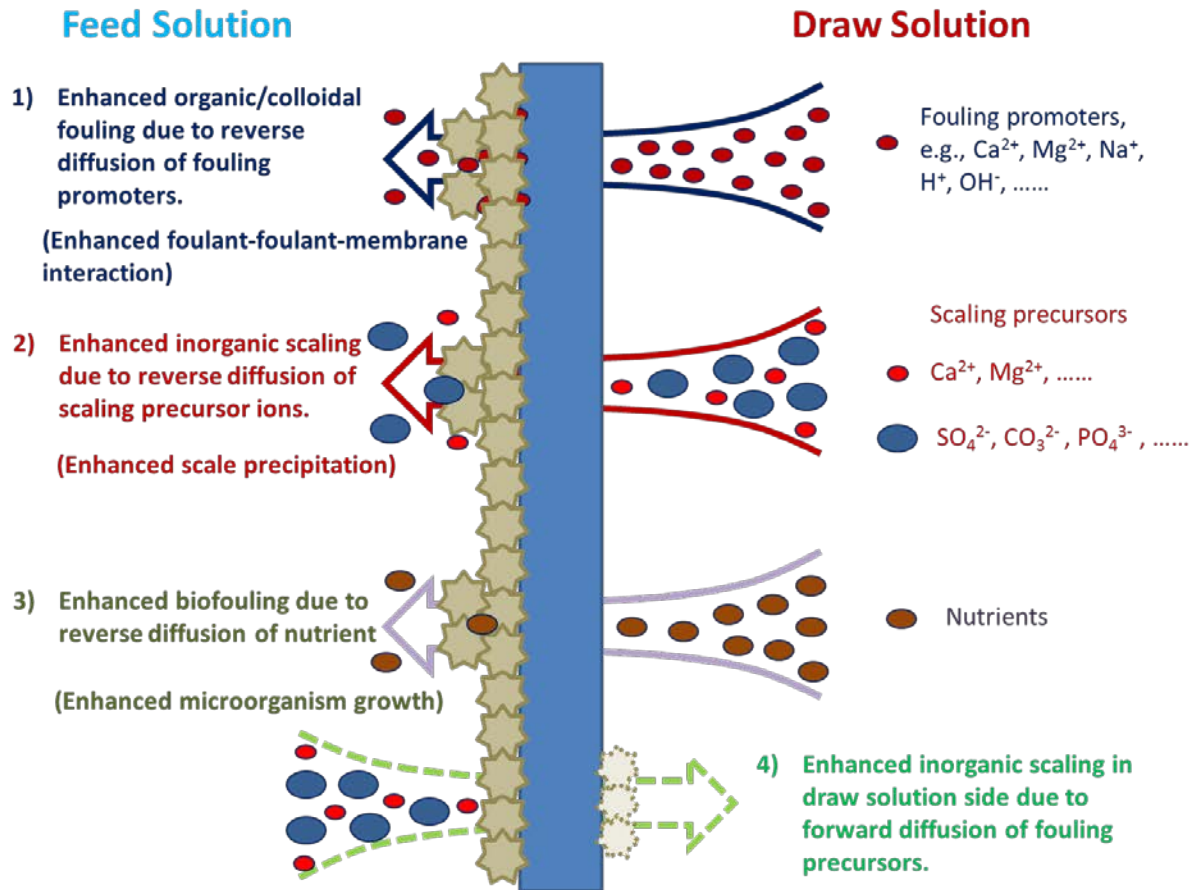


Figure 6. Schematic illustration of role of reverse solute diffusion (RSD) on enhanced membrane fouling in ODMPs.

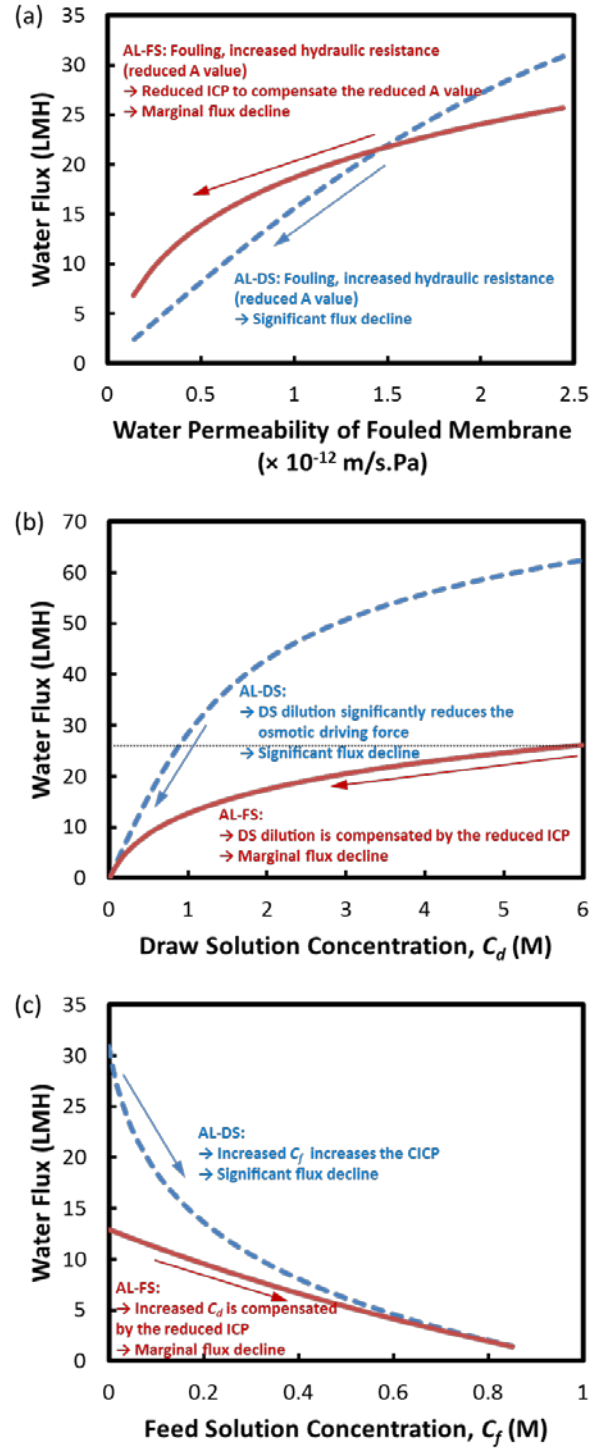


Figure 7. ICP self-compensation effect for the AL-FS orientation in different scenarios. (a) In the scenario of membrane fouling where water permeability is reduced. In the simulation, DS concentration is 5 M for AL-FS orientation and 1 M for AL-DS orientation respectively. (b) In the scenario of reduced DS concentration. (c) In the scenario of increased FS concentration. Other parameters for simulation: A value 2.14×10^{-12} m/s.Pa, B value 1.76×10^{-7} m/s, S value $456 \mu\text{m}$, $\Delta P = 0$ bar, $C_{ds} = 1$ M, and $C_{fs} = 10$ mM. Similar simulation was reported in ref. [27].

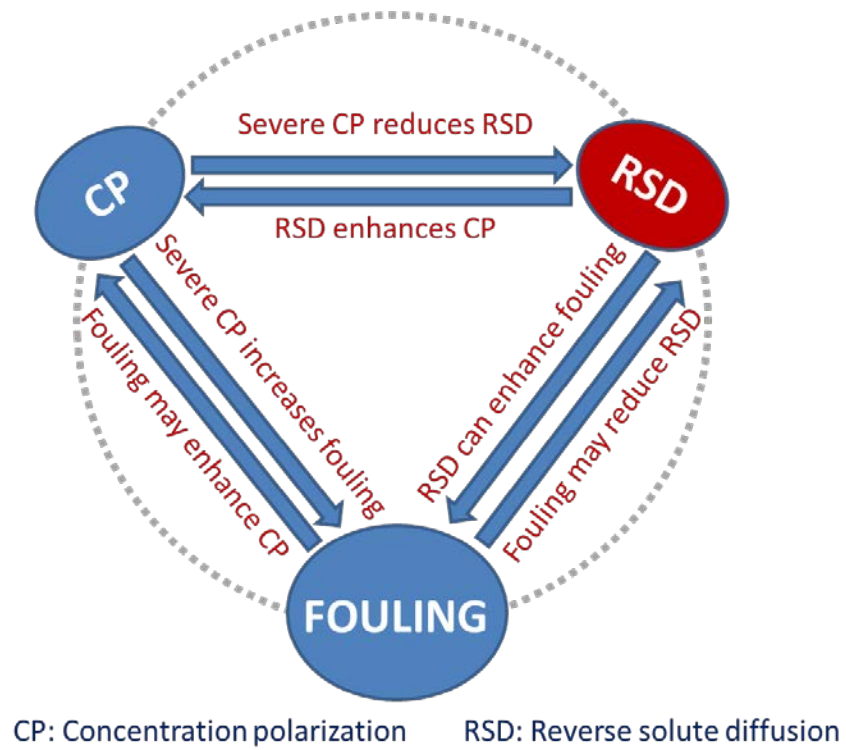
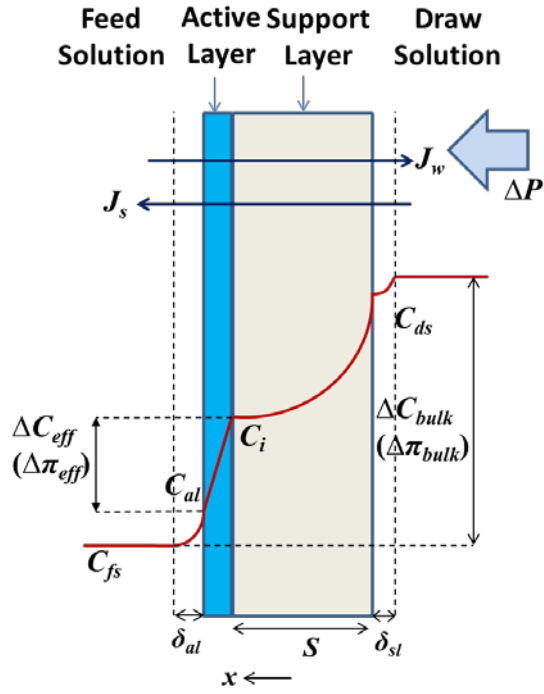


Figure 9. The intrinsic interrelationship among membrane fouling, concentration polarization (CP) and reverse solute diffusion (RSD) in ODMPs.

(a)

**AL – FS Orientation**

(b)

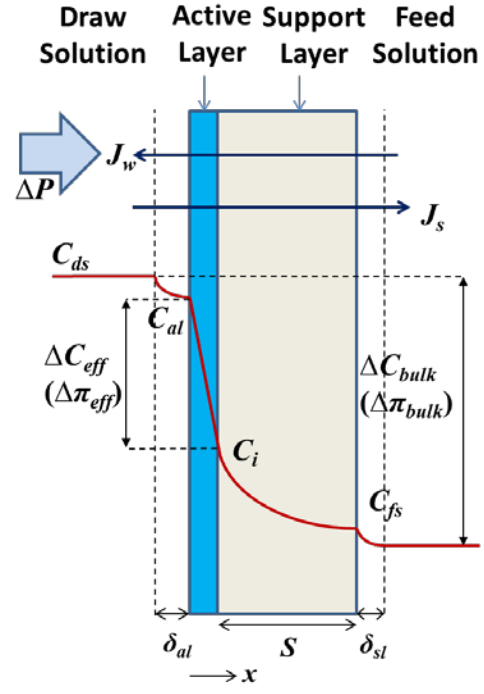
**AL – DS Orientation**

Figure A1. Concentration profile across the membrane due to ICP and ECP. Assuming the draw solution and feed solution contain the same solute.

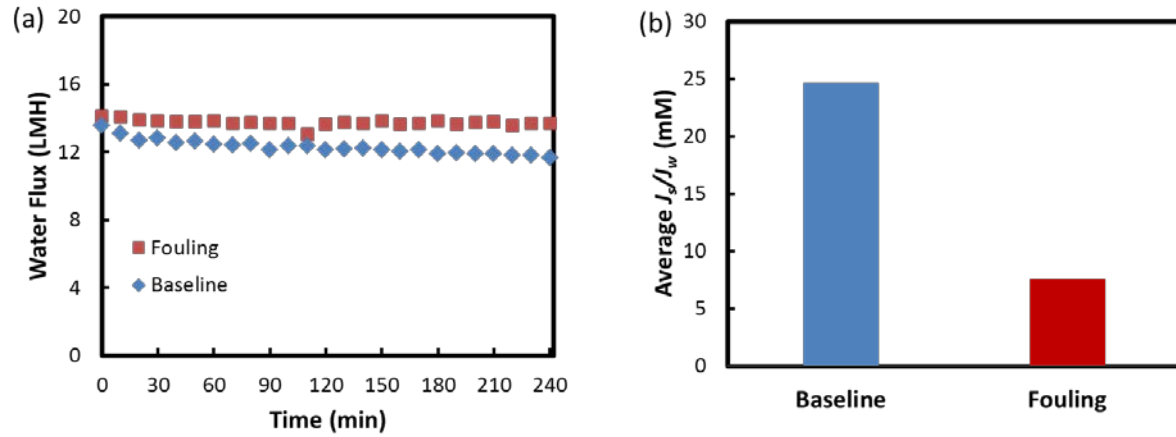


Figure B1. Enhanced water flux in humic acid fouling test due to fouling-reduced concentration polarization (CR-CP). (a) water flux in baseline test and humic acid fouling test in FO process, and (b) the average J_s/J_w in baseline test and fouling test. Fouling experimental conditions: feed solution only contained 10 mg/L humic acid in DI water, draw solution 0.5 M NaCl, cross-flow velocity 23.2 cm/s, AL-FS membrane orientation, and hand-casted TFC-PA FO membrane (the properties are reported in ref. [156]). In baseline test, DI water was used as feed solution.